Fusion of coherent-solitonic states

N. Korneev[a], E. Francisco[a], and V. Vysloukh[b]

[a]*Optics Department, Instituto Nacional de Astrofísica, Óptica y Electrónica, 1 Luis Enrique Erro, Tonantzintla, 72840, Pue., México.*

[b]*Universidad de las Américas, Ex-Hacienda Santa Catarina Mártir, San Andrés Cholula, 72810, Pue., México.*

Received 22 February 2024; accepted 13 November 2024

We report numerical results on the interaction between lowest order solutions of the Gross-Pitaevskii equation, the coherent-solitonic states. It is shown that under specific conditions two zero-order states can almost fuse into a first-order state and nearly maintain the shape during propagation. The conditions of fusion are analyzed. To a lesser extent, the same behavior is observed for three state fusion.

Keywords: Gross-Pitaevskii equation; Coherent-solitonic states; solitons; interaction; fusion.

DOI: https://doi.org/10.31349/RevMexFis.71.021302

1. Introduction

Solitons are solitary waves whose shape and velocity remain unchanged even after collisions between them. There are several nonlinear equations that admit solutions of solitonic type, in particular the nonlinear Schrödinger equation (NLSE) and the Korteweg-de Vries equation (KdV), which are known to be exactly integrable [1]. Solitons are present in many fields of science, including optics, plasmas, condensed matter physics, fluid mechanics, particle physics [2] and even in biological sciences. Their study has continuously motivated both theoretical and experimental research [3]. Optical solitons are wavepackets self-trapped in space, time, or both, which may arise when light propagates in nonlinear media. The NLSE models media with Kerr nonlinearity.

Another nonlinear model is the Gross-Pitaevskii equation (GPE),

$$i\frac{\partial\psi}{\partial t}+\frac{1}{2}\frac{\partial^2\psi}{\partial x^2}-\frac{1}{2}x^2\psi+\beta|\psi|^2\psi=0. \qquad (1)$$

It is used to describe phenomena such as Bose-Einstein condensates (BEC) [4, 5] and propagation of light in nonlinear waveguides. Here $\psi(x,t)$ is a wavefunction that depends on a transverse coordinate x and t, which can represent either a propagation coordinate or time. β is the nonlinearity constant, which is positive for a self-focusing medium, or negative for a self-defocusing medium.

It is currently unknown whether the GPE is integrable or not. This is a subject of ongoing research [6]. Several authors have proposed particular solutions, both analytical and numerical, to the GPE [7, 8].

A family of solutions called coherent-solitonic states (CSS), which combine properties of both solitons and coherent states of the quantum harmonic oscillator, was proposed in Ref. [9]. The mathematical expression for these states is [10]

$$\psi(x,t)=\exp\bigg[-ixq\sin(t)+i\frac{q^2}{2}\sin(t)\cos(t)-i\frac{\nu}{2}t\bigg]\phi(y), \qquad (2)$$

where $y=x-q\cos(t)$ is the coordinate in the oscillating frame, q is a real constant defining the initial wave packet shift, ν is the phase velocity and $\phi(y)$ is a real function that represents the profile of $\psi(x,t)$.

Substituting Eq. (2) into Eq. (1) yields [9]

$$\phi''-y^2\phi+2\beta\phi^3=-\nu\phi, \qquad (3)$$

where ϕ'' is the second derivative with respect to y. A symmetric profile satisfies $\phi_s(0)=h$, $\phi_s'(0)=0$, while an antisymmetric one satisfies $\phi_a(0)=0$, $\phi_a'(0)=h$.

When $\beta=0$, Eq. (3) becomes the Hermite equation which has solutions that decrease as $x\longrightarrow\pm\infty$ for $\nu_n=2n+1$, with $n=0,1,2,....$ However, when $\beta\neq 0$, the eigenvalues ν for which localized solutions exist depend on both β and the eigenfunction amplitude.

The stability analysis of coherent-solitonic states was presented in Ref. [11]. It was shown there that CSS of zeroth and first order are linearly stable. However, higher order solutions can develop linear instabilities in a certain range of CSS amplitude for a fixed nonlinearity value.

Various types of soliton interactions are known in the literature. For the integrable nonlinear Schrödinger equation (cubic NLSE), solitons retain their amplitudes and velocities after collisions, but their phases and positions can change [12]. Studies of the interaction between two solitons in waveguides have shown that they can undergo attractive and repulsive forces, steering, as well as merging into another soliton. These effects strongly depend on the relative phase between solitons. Depending on whether they are in phase or out of phase, attraction and fusion, or repulsion can be achieved [13–15]. In addition to phase, these phenomena also depend on the soliton's separation [16].

Some nonlinear equations that have single soliton solutions may also allow for other kinds of stable solutions, such as soliton molecules and hybrid solutions [17]. Soliton molecules are formed by the interaction of individual solitons. Bound states of two and three solitons in optical fibers have been observed [18]. The NLSE also admits the two-soliton solution and soliton molecules. For this case, it has been found that solitons in molecules may coalesce periodically resulting in a non-constant separation between them [19]. For some variants of the Gross-Pitaevskii equation, the possibility of soliton molecule formation has been suggested [20].

CSS's for nonzero nonlinearity can be regarded as solutions of solitonic type, and it is interesting to investigate how they interact. Here we study numerically the interaction between two and three coherent-solitonic states of zero order. It is shown, that two properly separated out-of-phase CSS's can form a single state, similar to the first-order CSS. It propagates nearly retaining its form. However, fusion is only possible for positive nonlinearity and for separations smaller than a certain critical value. We also show that three zero-order CSS's can form a state that closely resembles a second-order CSS.

2. Interaction of zero-order CSS

Solving Eq. (3) numerically yields the initial profile $\psi(x,0) = \phi(x-q)$. We use the initial condition $\phi(0) = h$, $\phi'(0) = 0$, and choose ν corresponding to zero-order CSS to ensure that the solution diminishes to zero for large x and does not exhibit any zero crossings.

Evolution of the wavefunction is obtained using the Galerkin method [6, 9, 11]. The function $\psi(x,t)$ is expanded as a sum of Hermite harmonics with time-dependent coefficients,

$$\psi(x,t) = \sum_{k=0}^{N} C_k(t) H_k(x), \tag{4}$$

where $H_k(x)$ is a k-th order Hermite function and N is the number of harmonics considered to achieve sufficient precision (typically $N = 40$). The initial profile is used to calculate the coefficients for $t = 0$ and the solutions for $t > 0$ are obtained using the Runge-Kutta method.

The q parameter indicates the initial shift of the zero time profile, $\phi(x-q)$. When $q = 0$, rectilinear propagation is observed; when $q \neq 0$, the solution exhibits transversal oscillation. Figure 4 shows the typical profiles of two shifted zero-order CSS (dashed lines) and that of a first-order CSS. In Fig. 6 the initial profile of a second-order CSS (thick line) is shown. An exact CSS maintains the same profile under propagation, but generally profiles of superposition of some CSSs will vary with time due to nonlinearity.

To simulate interactions between two zero-order CSS, we calculate $C_k(0)$ for each of two initial profiles, $\phi(x-q_1)$ and $\phi(x-q_2)$. If needed, coefficients corresponding to one of the profiles can be multiplied by a complex exponential to introduce a relative phase. Resulting coefficients after summation are used as the initial condition.

The first case studied corresponds to the interaction between two CSS symmetrically displaced from the center, $q_1 = -q_2 = 1$. The way in which this system evolves depends mainly on the relative phase shift between them, θ. Figure 1 shows the evolution for $h = 0.5$ and three relative phases. For $\theta = 0$, waves tend to interfere constructively in some regions at the center. For $\theta = \pi$, waves tend to repel and maintain their separation along propagation. For intermediate relative phases, the evolution becomes more complex [Fig. 1b)].

Another case studied is the interaction between a non-shifted zero-order CSS and a shifted one, $q_1 = 0$ and $q_2 = 1$. This case is shown in Fig. 2.

For longer propagation times, the general behavior does not change considerably, but slight variations are observed.

To investigate the periodicity, we fix a specific transversal coordinate, x, and calculate $|\psi(x,t)|$ as a function of t. The separation between successive minima of this function varies, the function is not perfectly periodic. The average of these separations gives an estimate of the period. We have averaged over ranges of 20π and 40π with similar results. Figure 3 shows the difference between half the average period T and π as a function of h for three different symmetrical shifts q. The sign of h indicates the sign of nonlinearity ($\beta = 1$ for positive, and $\beta = -1$ for negative). It is observed that the

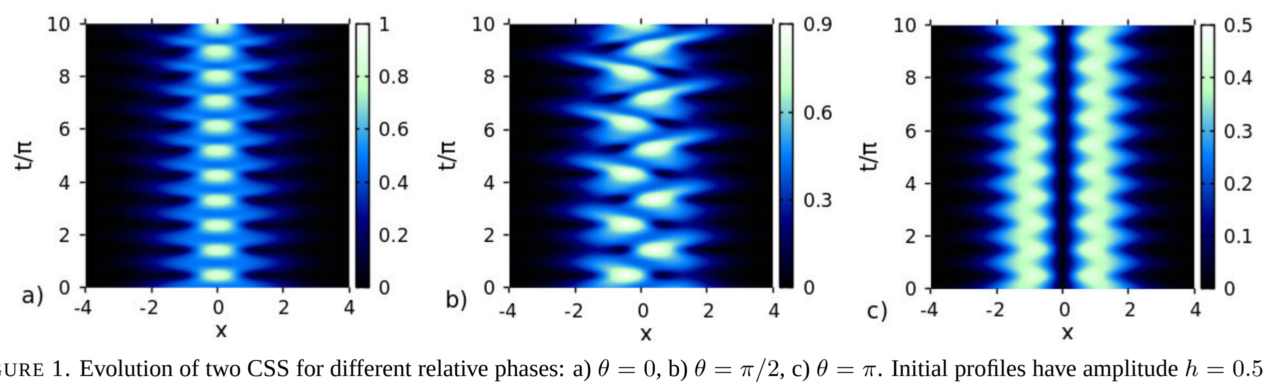

FIGURE 1. Evolution of two CSS for different relative phases: a) $\theta = 0$, b) $\theta = \pi/2$, c) $\theta = \pi$. Initial profiles have amplitude $h = 0.5$ and a symmetric shift of $q = \pm 1$; the nonlinearity is $\beta = 1$. All plots have the same time scale. Color bars indicate the magnitude $|\psi(x,t)|$.

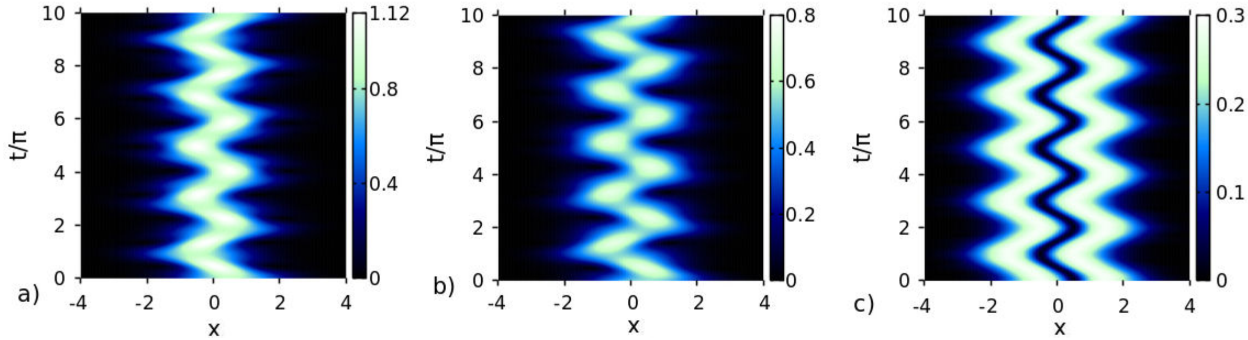

FIGURE 2. Evolution of two non-symmetrically shifted zero-order CSS for relative phases: a) $\theta = 0$, b) $\theta = \pi/2$, c) $\theta = \pi$, with amplitudes $h = 0.5$. One profile is initially centered, $q_1 = 0$, and the other one is displaced by $q_2 = 1$; the nonlinearity is $\beta = 1$.

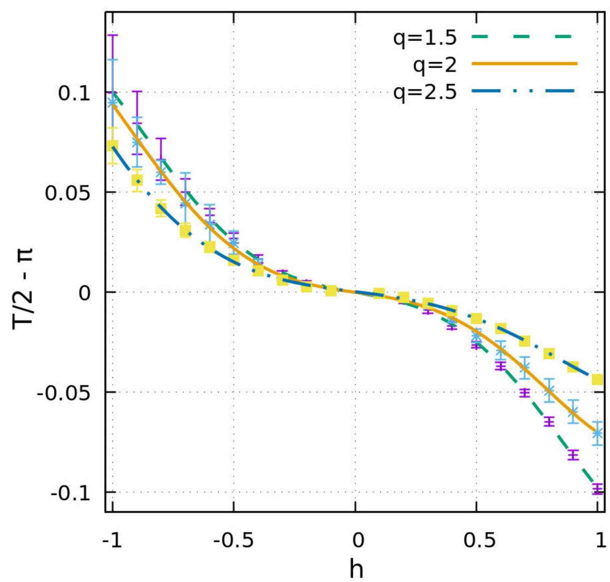

FIGURE 3. Difference between half the characteristic period T and π in function of h for three values of q. For zero nonlinearity ($h \longrightarrow 0$), the half period is exactly π. Estimates of the period have been carried out at $x = 1.5$. Standard deviation σ is larger for negative nonlinearity.

nonlinear interaction modifies the period; it is larger for negative nonlinearity and smaller for positive one. From the set of such separations, we have computed the standard deviation, σ, as an indication of the variation in period. In Fig. 3, the values of σ are represented by error bars.

3. Fusion of two and three zero-order CSS

It is well known that solitons can attract and fuse together for $\theta = 0$, while they repel (or steer) each other for $\theta = \pi$. Simulations show that CSS can exhibit a similar behavior under certain conditions. However, the repulsion between zero-order CSS can be harnessed to fuse them into CSS of higher orders. Indeed, some zero-order CSS, symmetrically displaced from the origin, may form a profile which resembles that of a CSS of higher order and the bound state propagates very similar to the latter. We investigate this effect for interactions of two and three zero-order CSS.

In the first case, two zero-order CSS, with a relative phase of $\theta = \pi$ between them and symmetrical shifts from the origin ($-q$ and q), may form a profile very close to that of a

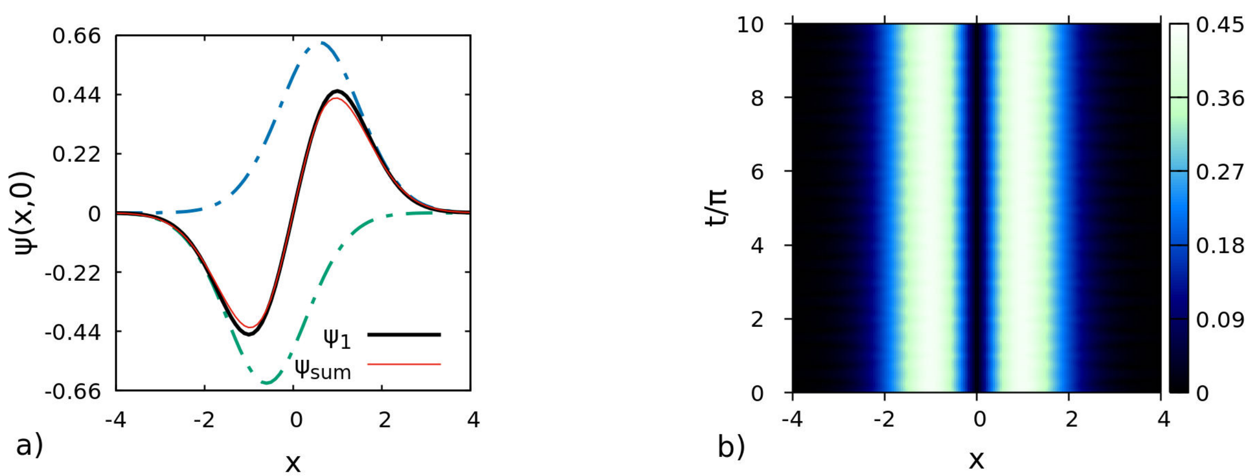

FIGURE 4. Fusion of two zero-order CSS with $q = 0.6$ and $h_0 = 0.633$. a) Profiles of the sum of two zero-order CSS's (red) and corresponding first-order CSS (black), $h_1 = 0.73341$. The dashed lines represent initial profiles of zero-order CSS, symmetrically shifted from the origin by $\pm q$, the sum of which yields the profile in red. b) Propagation of the sum of two zero-order CSS.

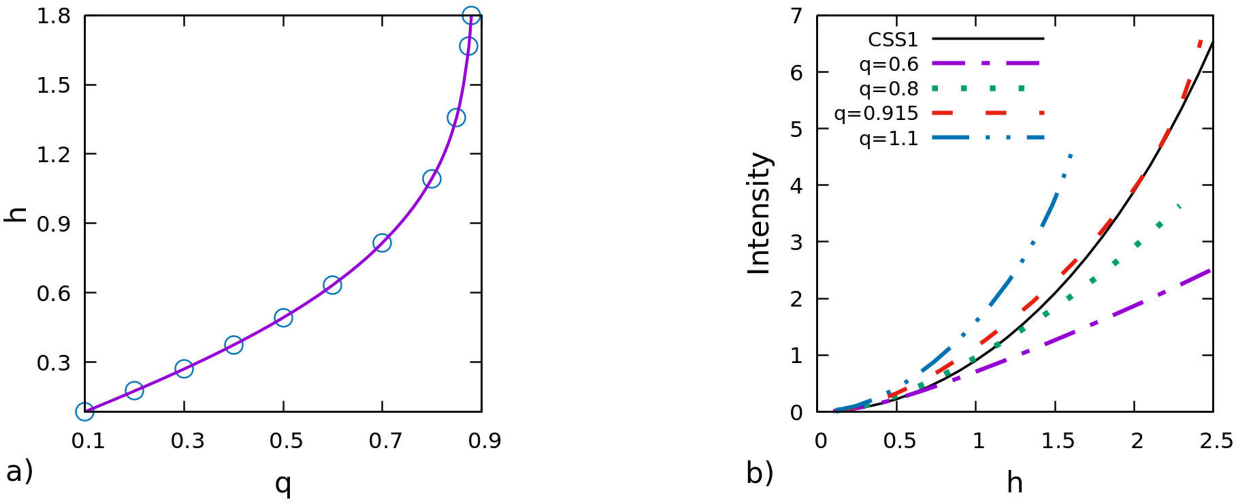

FIGURE 5. a) Optimal values for h and q to get best approximations to a first-order CSS lay on this curve, critical value of q is around 0.89. b) Intensity vs h curves for different shifts q. The dashed lines correspond to fusion profiles, the solid line corresponds to a pure CSS of the first order.

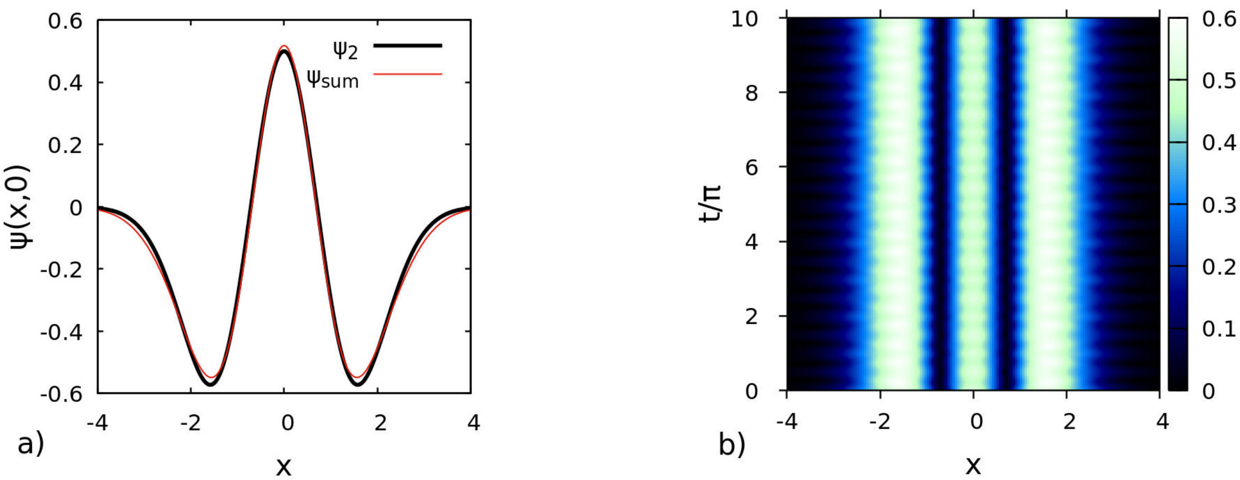

FIGURE 6. a) Comparison of profiles: ψ_2 is the exact second-order CSS for $h = 0.5$; ψ_{sum} is the sum of three zero-order CSS (fusion) for parameters $h_c = 1.130688$, $h_s = 0.789475$ and $q = 1.219687$, computed by an optimization algorithm. b) Propagation pattern of the fusion profile.

first-order CSS. Figure 4 shows the two profiles together and the propagation pattern of the system. Its resemblance to that of a pure first-order CSS depends on parameters h and q.

For each value of q, the closest profile is attained at a particular value of h. This allows to find pairs (q, h) of maximal resemblance. To find these pairs, we calculate the squared width of $\psi(x, t)$ as a function of time:

$$\Delta x(t) = \frac{\int x^2 |\psi(x,t)|^2 dx}{\int |\psi(x,t)|^2 dx}. \tag{5}$$

For a pure CSS, $\Delta x(t)$ is constant. The propagation of a combined state results in an oscillating function. So, within an interval of some periods we searched for the extrema of Δx in function of t and calculated the quantity $\delta = |\Delta x_{\max} - \Delta x_{\min}|$. Then, for a fixed value of q, the value of h which minimizes δ corresponds to the maximal resemblance. The plot of these best choices (q, h) [Fig. 5a)] suggests that there exists a critical value of q, *i.e.*, q does not surpass a certain limit. The best resemblance is obtained for small values of q and h, which corresponds to the fact that the first derivative of the zero-order Hermite function is proportional to the first-order Hermite function.

To understand the origin of the critical value of q we assume that the derivative of the zero-order CSS superposition at $x = 0$ should give the value of an analogous h parameter for first-order CSS, h_{fusion}. We also can calculate the total intensity of the wavefunction by integrating $|\psi(x, 0)|^2$ along the x- axis. We characterize a fusion profile by plotting the intensity I_{fusion} against h_{fusion} for different q values [Fig. 5b)]. The dependence crosses the corresponding curve for first-order CSS at a point that approximately corresponds to the correct parameter h for first-order CSS. The fusion curves do not cross the corresponding CSS curve at all for q values greater than the critical value 0.915, which is reasonably close to the critical value of 0.89 suggested by Fig. 5a).

It is not possible to obtain fusion of this type for negative nonlinearity.

Similarly, three zero-order CSS may fuse into a second-order CSS. In this case, one zero-order CSS must be centered, while the other two are symmetrically shifted from the origin (by $-q$ and q). Additionally, there must be a relative phase of $\theta = \pi$ between the central CSS and the side ones.

In this case the resemblance between the resultant profile and that of a pure second-order CSS is less pronounced than for two CSS fusion. Moreover, the approach now depends on three parameters: the amplitudes of zero-order CSS at the center, h_c, and sides, h_s, as well as the absolute value of the shift, q.

For this case, an optimization process is suggested, where the integral

$$\int \left[\phi(x; h_c, h_s, q) - \Phi_2(x)\right]^2 dx, \tag{6}$$

is minimized. Here, $\Phi_2(x)$ represents the profile of a second-order CSS, and $\phi(x; h_c, h_s, q)$ is the initial profile obtained from the sum of three zero-order CSS. Note that this function has parameters h_c, h_s and q, and the final values should be found using the optimization procedure from an already close profile. Figure 6 shows the resemblance between profiles and the propagation pattern for this case.

4. Discussion and conclusions

Using computer simulations we have uncovered an interesting effect: two (or three) CSSs of zero order can form a stable state, similar to a CSS of higher order (first or second). We interpret this effect in terms of a stable balance between repulsion of two out-of phase solitons and compression due to a parabolic potential. For the case of two CSS, the numerical experiment allows to establish the range of parameters (amplitudes and initial shifts) where this balance is possible.

We have demonstrated in principle the possibility of forming the second-order CSS from three CSS of the order zero. The detailed investigation of this case is beyond the scope of this paper.

1. M. J. Ablowitz and H. Segur, Solitons and the Inverse Scattering Transform (Society for Industrial and Applied Mathematics, 1981), `https://doi.org/10.1137/1.9781611970883`.
2. Z. Chen, M. Segev, and D. N. Christodoulides, Optical spatial solitons: historical overview and recent advances, *Reports on Progress in Physics* **75** (2012) 086401, `https://doi.org/10.1088/0034-4885/75/8/086401`.
3. B. A. Malomed, Two-Dimensional Solitons in Nonlocal Media: A Brief Review, *Symmetry* **14** (2022) 1565, `https://doi.org/10.3390/sym14081565`.
4. L. Pitaevskii and S. Stringari, Bose-Einstein Condensation, in: International Series of Monographs on Physics (Clarendon Press, 2003), `https://books.google.com.mx/books?id=rIobbOxC4j4C`.
5. C. Barenghi and N. Parker, A Primer On Quantum Fluids, in: SpringerBriefs in Physics (Springer International Publishing, 2016), `https://books.google.com.mx/books?id=kGLJjwEACAAJ`.
6. T. Bland *et al.*, Probing quasi-integrability of the Gross-Pitaevskii equation in a harmonic-oscillator potential, *J. Phys. B: At. Mol. Opt. Phys.* **51** (2018) 205303, `https://doi.org/10.1088/1361-6455/aae0ba`.
7. C. Trallero-Giner *et al.*, Formal analytical solutions for the Gross-Pitaevskii equation, *Physica D: Nonlinear Phenomena* **237** (2008) 2342, `https://doi.org/10.1016/j.physd.2008.02.017`.
8. W. Bao, D. Jaksch, and P. A. Markowich, Numerical solution of the Gross-Pitaevskii equation for Bose-Einstein condensation, *Journal of Computational Physics* **187** (2003) 318, `https://doi.org/10.1016/S0021-9991(03)00102-5`.
9. N. Korneev and V. Vysloukh, Coherent-solitonic states for Gross-Pitaevskii equation with parabolic potential, *Optik* **255** (2022) 168628, `https://doi.org/10.1016/j.ijleo.2022.168628`.
10. J. Gazeau, Coherent States in Quantum Physics (Wiley, 2009), `https://books.google.com.mx/books?id=tJhevgAACAAJ`.
11. N. Korneev, E. Francisco, and V. Vysloukh, Stability of coherent-solitonic states for Gross-Pitaevskii equation with parabolic potential, *Physics Letters A* **490** (2023) 129201, `https://doi.org/10.1016/j.physleta.2023.129201`.
12. Y. S. Kivshar and G. P. Agrawal, Chapter 2 - Spatial Solitons, Optical Solitons (Academic Press, Burlington, 2003), `https://doi.org/10.1016/B978-012410590-4/50002-4`.
13. S. R. Friberg, Soliton fusion and steering by the simultaneous launch of two different-color solitons, *Opt. Lett.* **16** (1991) 1484, `https://doi.org/10.1364/OL.16.001484`.
14. F. M. Mitschke and L. F. Mollenauer, Experimental observation of interaction forces between solitons in optical fibers, *Opt. Lett.* **12** (1987) 355, `https://doi.org/10.1364/OL.12.000355`.
15. Y. Kodama and K. Nozaki, Soliton interaction in optical fibers, *Opt. Lett.* **12** (1987) 1038, `https://doi.org/10.1364/OL.12.001038`.
16. Z. Fengwu and Y. Jiaren, Interaction Between Two Nonlinear Schrödinger Solitons, *Chinese Physics Letters* **11** (1994) 265, `https://doi.org/10.1088/0256-307X/11/5/003`.

17. H. Ma, H. Huang, and A. Deng, Soliton molecules, asymmetric solitons and hybrid solutions for KdV-CDG equation, *Partial Differential Equations in Applied Mathematics* **5** (2022) 100214, https://doi.org/10.1016/j.padiff.2021.100214.

18. P. Rohrmann, A. Hause, and F. Mitschke, Two-soliton and three-soliton molecules in optical fibers, *Phys. Rev. A* **87** (2013) 043834, https://doi.org/10.1103/PhysRevA.87.043834.

19. K. Mohammed Elhadj *et al*., Singular soliton molecules of the nonlinear Schrödinger equation, *Phys. Rev. E* **101** (2020) 042221, https://doi.org/10.1103/PhysRevE.101.042221.

20. U. Al Khawaja, Stability and dynamics of two-soliton molecules, *Phys. Rev. E* **81** (2010) 056603, https://doi.org/10.1103/PhysRevE.81.056603.